

## Percolation of finite-sized objects on a lattice

R. E. Amritkar<sup>1</sup> and Manojit Roy<sup>2</sup>

<sup>1</sup>Physical Research Laboratory, Navrangpura, Ahmedabad 380 009, India

<sup>2</sup>Department of Physics, University of Pune, Pune 411 007, India

(Received 18 August 1997)

We study the percolation of *finite-sized* objects on two- and three-dimensional lattices. Our motivation stems, on one hand, from some recent interesting experimental results on transport properties of impurity-doped oxide perovskites, and on the other hand from the theoretical appeal that this problem presents. Our system exhibits a well-defined percolation threshold. We estimate the size of magnetic polarons, believed to be the carriers of the above-mentioned transport. We have also obtained two critical exponents for our model, which characterize its universality class. [S1063-651X(98)06801-9]

PACS number(s): 64.60.Ak, 64.60.Fr, 71.38.+i

Over the last couple of decades percolation theory has generated lot of interest, both from theoretical as well as applicational points of view [1–12]. Percolation is an important model exhibiting a second order phase transition with the associated critical exponents [1,4,5]. It has also been successfully applied to transport and phase transitions in several physical systems in the presence of voids or impurities [1,6,7,11,12]. In this paper we investigate the percolation mechanism of objects *with finite spatial extent* on a lattice. To the best of our knowledge this problem has not been studied so far.

We are motivated for this type of study for the following reasons. Firstly, the problem has interesting physical application. Recent experimental investigations in transport properties of Fe-doped  $\text{La}_{0.75}\text{Ca}_{0.25}\text{MnO}_3$  ceramics [13] have thrown important light on the role of magnetic polarons that are finite-sized objects [14–16]. In the lattice the Fe ions occupy the Mn sites. There is a jump in the resistivity of the system by a factor of about 80 at about 4% concentration of the Fe ions. Observations of isomer shift indicate that Fe ions are in the 3+ state only and hence cannot be expected to act as a double exchange partner for the  $\text{Mn}^{4+}$  ions. Thus the Fe impurities will be prohibiting the transport of polarons. Using this physical picture the jump in resistivity may be interpreted as a percolation transition for the polarons. Secondly, our problem has its own theoretical appeal, which merits a thorough study. It is interesting to ask whether finiteness of size has any effect on critical exponents and hence on universality classes. Finally, our model may have interesting application in the transport problem of vehicles of different sizes in a randomly grown habitation. The last problem has an additional feature that not only the objects themselves but also the obstacles have finite sizes. We shall see that in some cases the two problems can be mapped into each other.

Our observations bring out a well-defined percolation threshold probability for our model in both two and three dimension. We have analyzed our results using the ansatz of scaling due to the finite lattice size. We also estimate some critical exponents near the threshold.

The model we consider is as follows. We take a lattice and randomly disallow its sites with a probability  $q$ . We define our percolating object as a spatially extended entity of linear dimension  $r$  (in lattice units) consisting of  $n(r)$  sites.

We now say that such an object is allowed to percolate in the lattice only if none of its  $n(r)$  sites overlaps with any of the disallowed sites. We then study the standard percolation problem for such an object.

One can also study the following complementary problem. Let us place obstacles of linear size  $r$  containing  $n(r)$  sites with a suitably defined center at random locations with probability  $q$ . We now treat the remaining sites as allowed and study the standard site percolation problem for point objects. It is easy to see that the two problems are essentially equivalent under the following conditions: firstly, the centers of the finite-sized objects or obstacles lie on a site; secondly, the objects or obstacles themselves have the same symmetry as that of the underlying lattice; and finally, the obstacles are allowed to overlap [17]. Numerically it is easier to study the problem with obstacles, which we use for calculations in this paper.

We now present our main results [18]. We consider a two-dimensional square lattice and a three-dimensional simple cubic lattice for our study. We restrict ourselves to the cases of objects with circular symmetry in two dimensions and spherical symmetry in three dimensions, with  $r$  as radius and center on a lattice site. We have used periodic boundary conditions for our system (otherwise finite-sized objects are ill defined at and near the lattice boundary). Different linear sizes  $L$  of the lattice are considered: for two dimensions, we have taken  $L=10,20,40,80,160,320,640,1280,2560$ , and 5120, and for three dimensions,  $L=10,20,40,80,160$ , and 250. We have varied probability  $q$  between 0 and 1, and also used different values of the radius  $r$  (first column of Table I shows various  $r$  values for two-dimensional lattice), starting with the nearest neighbor case ( $r=1$  lattice unit). Data are averaged over many realizations of randomly generated disallowed sites for each value of  $q$ . It is to be noted that no exact analysis is possible for our model in two or three dimensions, though some exact results can be obtained for one-dimensional lattice and Bethe lattice [19].

We define a *cluster* as a group of sites with the following properties: centers of the percolating objects can be placed on these sites, and these sites are connected through their nearest neighbors. We call a lattice *percolating* for a given  $q$  and  $r$  when there exists at least one cluster spanning the

TABLE I. The quantities  $n(r)$ , the number of sites in an object,  $q_c$ , the threshold probability,  $p(q_c, r)$ , the probability for the allowed sites for the center of an object at  $q_c$ , and  $\beta$  and  $\gamma$ , the critical exponents, for different radii  $r$  in a two-dimensional square lattice. Error margins for  $q_c$ ,  $\beta$ , and  $\gamma$  are  $\pm 0.0001$ ,  $\pm 0.01$ , and  $\pm 0.1$ , respectively. Values for point object ( $r=0$ ) are from Ref. [1].

$r$	$n(r)$	$q_c$	$p(q_c, r)$	$\beta$	$\gamma$
0	1		0.5928	0.14	2.39
1	5	0.1153	0.5420	0.14	2.30
$\sqrt{2}$	9	0.0868	0.4417	0.14	2.29
2	13	0.0538	0.4873	0.15	2.22
$\sqrt{5}$	21	0.0406	0.4188	0.15	2.28
$\sqrt{8}$	25	0.0358	0.4020	0.14	2.39

lattice end to end (a so-called ‘‘infinite cluster’’). We define *threshold probability*  $q_c$  such that for  $q > q_c$  the lattice ceases to be percolating. It is obvious that  $q_c$  is a function of the radius  $r$ .

Let  $F(q)$  denote the fraction of percolating realizations (those that support a spanning cluster). Figures 1 and 2 show, respectively, for two and three dimensions, the variation of  $F(q)$  with the probability  $q$ , for different lattice sizes  $L$  and radius  $r=1$ . Both plots exhibit an approach towards a step function of the form

$$F(q) = \begin{cases} 1 & \text{for } q < q_c, \\ 0 & \text{for } q > q_c, \end{cases} \quad (1)$$

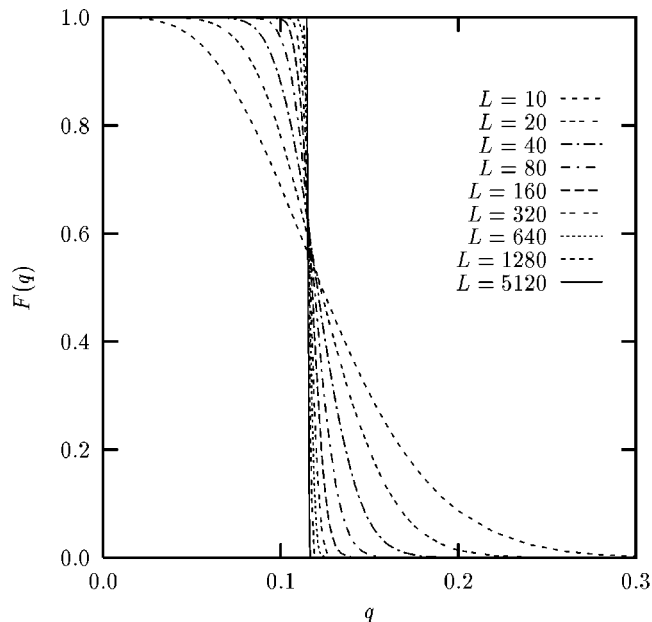


FIG. 1. Variation of the percolating fraction  $F(q)$  is plotted against the probability  $q$ , for lattice sizes  $L=10, 20, 40, 80, 160, 320, 640, 1280$ , and  $5120$ , and with radius  $r=1$  (lattice unit), for a two-dimensional square lattice (plot for  $L=2560$  is not shown for the sake of clarity). Data are averaged over 100 000 realizations for  $L=10$ , 50 000 for  $L=20$ , 20 000 for  $L=40$ , 10 000 for  $L=80$ , 5000 for  $L=160$ , 2000 for  $L=320$ , 1000 for  $L=640$ , 500 for  $L=1280$ , and 50 for  $L=5120$ .

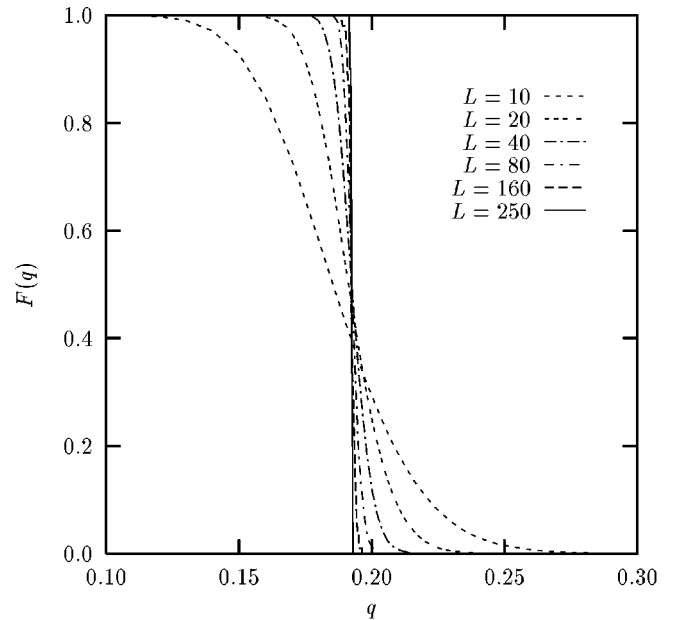


FIG. 2.  $F(q)$  vs  $q$  plot for a three-dimensional simple cubic lattice, for  $L=10, 20, 40, 80, 160$ , and  $250$ , with  $r=1$ . Realizations taken are 100 000 for  $L=10$ , 30 000 for  $L=20$ , 10 000 for  $L=40$ , 2000 for  $L=80$ , 200 for  $L=160$ , and 10 for  $L=250$ .

as  $L$  increases to  $\infty$ . This behavior remains essentially the same for all other values of  $r$  that we have considered. The data of both Fig. 1 and Fig. 2 are seen to obey a finite-(lattice) size scaling relation, near the threshold  $q_c$ , of the type

$$F(q, L) \rightarrow L^{-b} G(L^a |q - q_c|), \quad (2)$$

where  $a$  and  $b$  are the scaling exponents. We have seen that all the graphs of Fig. 1 collapse onto a single function, which is almost a step function of the form (1), and the same is true for the graphs of Fig. 2. This confirms the existence of scaling behavior (2). We have obtained the exponents  $a$ ,  $b$  for various radii  $r$  in both dimensions. As  $r$  increases from 1 to  $\sqrt{8}$ ,  $a$  decreases monotonically from 0.8 to 0.7 for a two-dimensional square lattice, whereas for a three-dimensional simple cubic lattice it reduces from 1.17 to 0.96; the value of  $b$  remains zero for all  $r$  in both cases. We get an estimate of  $q_c$  using this scaling scheme, as  $L \rightarrow \infty$ . In the third column of Table I we list these values for all finite  $r$  for the two-dimensional lattice. There is one more way to obtain  $q_c$  as explained below. The graphs of Fig. 1 and Fig. 2 are approximately linear for values of  $F(q)$  between 0.3 and 0.6. We consider the  $q$  intercepts of these lines. The extrapolated value of this intercept as  $1/L \rightarrow 0$  yields  $q_c$ . These values are almost identical to those listed in Table I, thereby exhibiting internal consistency of our calculations.

One can calculate the probability  $p$  that a given lattice site is allowed to be the center of a percolating object. Quite simply, the required probability is

$$p(q, r) = (1 - q)^{n(r)}, \quad (3)$$

where  $q$  is our original probability and  $n(r)$  is the number of lattice sites contained in the object. The second column of Table I shows the values of  $n(r)$  for all  $r$ , in two dimensions.

TABLE II. The quantities  $n(r), q_c, p(q_c, r)$ , for different  $r$  values in a three-dimensional simple cubic lattice. Error margin for  $q_c$  is  $\pm 0.0001$ .  $p(q_c, r)$  for  $r=0$  is from Ref. [1].

$r$	$n(r)$	$q_c$	$p(q_c, r)$
0	1		0.3116
1	7	0.1921	0.2247
$\sqrt{2}$	19	0.0912	0.1625
$\sqrt{3}$	27	0.0752	0.1211
2	33	0.0591	0.1340
$\sqrt{5}$	57	0.0355	0.1274
$\sqrt{6}$	81	0.0285	0.0961
$\sqrt{8}$	93	0.0242	0.1025

We list, in the fourth column, the values of  $p(q_c, r)$  for different radii  $r$  at the threshold  $q_c$ .

Table II shows, for a three-dimensional simple cubic lattice, the various  $r$  values and the corresponding quantities  $n(r)$ ,  $q_c$ , and  $p(q_c, r)$ . We notice that for both two and three dimensions, the objects with finite  $r$  are percolating at lower  $p$  values than the point objects. The reason for this becomes clear if we look at the equivalent problem of obstacles. Here the sites are disallowed in clumps rather than in a homogeneous manner throughout the lattice, thereby leaving more channels open for percolation. This effect is more pronounced the higher the radius. For instance, in three dimensions one sees that for  $r = \sqrt{6}$  the lattice percolates even with the removal of more than 90% of its sites. This also brings out another interesting feature. The dependence of  $p(q_c, r)$  on  $r$  is not monotonous; it exhibits occasional peaks (in Table I one peak is at  $r = 2$ , and in Table II two peaks can be seen at  $r = 2$  and  $\sqrt{8}$ ).

As discussed in the Introduction, the jump in the resistivity of Fe-doped ceramic  $\text{La}_{0.75}\text{Ca}_{0.25}\text{MnO}_3$  at about 4% concentration of Fe ions may be interpreted as a percolation transition for the polarons. By assuming a homogeneous and uniform distribution of Fe ions, Ogale *et al.* have suggested that the polaron radius is about one lattice unit. However, the Fe ions are more likely to be randomly distributed in the lattice. This leaves many channels open for transport and thereby allows objects with bigger radii to pass through. Table II (for the three-dimensional case) indicates a  $q_c$  value of 0.04 for radius  $r$  between 2 and  $\sqrt{5}$ . This suggests a polaron radius slightly larger than two lattice units [20].

As in the standard percolation problem we find clusters of various sizes. We have investigated the distribution of maximum size  $S_m$  (normalized by the number of lattice sites) of the cluster, averaged over lattice realizations, for different values of  $q$  and  $r$ . Figure 3 plots the variation of  $S_m$  with  $q$ , for different lattice sizes and the radius  $r = 1$ , in a two-dimensional lattice. The plot exhibits a sharp fall at the threshold  $q_c$  for large  $L$ . This behavior remains essentially similar for all other values of  $r$ . A similar finite-size scaling behavior as for a percolating fraction  $F(q)$  [Eq. (2)] is observed for  $S_m$ . We have estimated the corresponding scaling exponents  $a$ ,  $b$ .  $a$  varies in essentially the same way in both the dimensions as stated before for the case of  $F(q)$ . The exponent  $b$ , however, has nonzero values:  $b = 0.14$  for a two-dimensional lattice, whereas  $b = 0.5$  for three dimensional

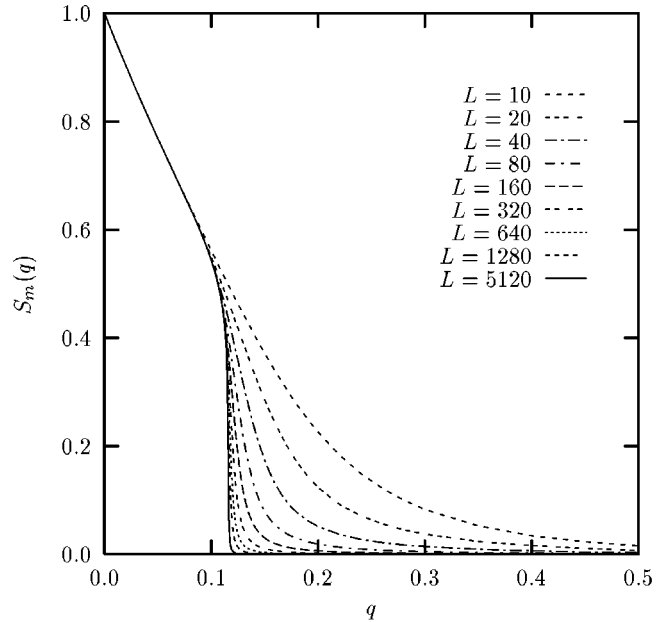


FIG. 3. Variation of the maximum size  $S_m(q)$  of the cluster is plotted against  $q$ , for the same  $L$  and  $r$  values as in Fig. 1.

lattice, independent of the radii  $r$ .

We have studied the nature of the decay of Fig. 3 near  $q_c$ . We observe this to be a *power law* of the form

$$S_m(q) \propto (q_c - q)^\beta. \quad (4)$$

We have estimated the exponent  $\beta$  of the relation (4) for both two- and three-dimensional lattices with different radii  $r$ . The fifth column of Table I lists the  $\beta$  values for different  $r$ , for the two-dimensional lattice. The error margin for our estimates is  $\pm 0.01$ . We have also included the corresponding exponent for point object (taken from [1]). We have not listed our  $\beta$  estimates for a three-dimensional lattice because the error margin was not within acceptable limit (the reason is that one has to explore lattice sizes larger than  $L = 250$ , which is the maximum size we could study due to limited computer resource [18]).

We have also studied the distribution of average size  $S_a$  of the clusters, excluding the infinite cluster, as  $q$  and  $r$  are varied. We define  $S_a$  following Stauffer *et al.* [1]. The probability that an arbitrary site belongs to any finite cluster in the lattice is  $\sum_s n_s s$ , where  $n_s$  is the number of the clusters of size  $s$ , normalized by the number of lattice sites. Then  $w_s = n_s s / \sum_s n_s s$  is the probability that the cluster to which an arbitrary allowed site belongs has a size  $s$ . The average size  $S_a$  is therefore

$$S_a = \sum_s w_s s = \sum_s \left( n_s s^2 / \sum_s n_s s \right). \quad (5)$$

As explained in Ref. [1], we take Eq. (5) as the definition of our mean size and not the more familiar expression  $\sum_s n_s s / \sum_s n_s$ , because in Eq. (5) lattice sites, rather than the clusters, are selected with equal probability. The average size  $S_a$  shows a diverging trend near  $q_c$  from both sides. It also exhibits finite-size scaling as for  $F(q)$  [Eq. (2)] and  $S_m$ . We have estimated the scaling exponents  $a$ ,  $b$  for  $S_a$ . We find

that  $a$  varies with  $r$  in the same way as in the earlier two cases of  $F$  and  $S_m$ . Exponent  $b$  takes the value  $-1.64$  in two dimensions,  $-1.7$  in three dimensions, irrespective of the radius  $r$ .

We have investigated the nature of divergence of  $S_a$  near the threshold  $q_c$ . We find it to be a *power law* of the type

$$S_a(q) \propto |q_c - q|^{-\gamma}, \quad (6)$$

where  $\gamma$  is the power-law exponent. In the last column of Table I we list the values of  $\gamma$  for various  $r$ , for a two-dimensional lattice. The corresponding error margin is  $\pm 0.1$ . We also show the value for point object case [1] for comparison. We have not shown the  $\gamma$  values for a three-dimensional lattice, for reasons stated earlier.

The question that remains to be answered is whether the universality class for our model, indicated by the exponents  $\beta$  and  $\gamma$ , is the same as, or distinct from, that of the point percolation case. The similarity of the values of  $\beta$  and  $\gamma$ , within their respective error margins, to their  $r=0$  counterparts may suggest these two to be the same. However, possibility exists that by taking larger lattice sizes and with consequent reduction in error one gets a quite distinct

universality class for finite-sized object case. Unfortunately, no definitive conclusion can be drawn at this stage.

In conclusion, we have, to our knowledge for the first time, investigated the percolation mechanism of finite-sized objects. We observe a well-defined percolating threshold for our model, in a two-dimensional square lattice and a three-dimensional simple cubic lattice, the threshold depending on the radius of the percolating objects. Based on this study, we have made an estimate of the size of polarons that are believed to be carriers of transport in oxide perovskites [21]. In our model there exists a scaling due to the finite size of the lattice, thereby allowing us to obtain important quantities for infinite systems from finite samples. We have also obtained two critical exponents, which characterize the universality class for our system. We expect that our model will be useful in characterizing the problem of transport of finite-sized objects, such as finite-sized excitations in solids and heavy vehicles in a randomly grown habitation.

One of the authors (R.E.A.) acknowledges the Department of Science and Technology (India) and the other (M.R.) acknowledges the University Grants Commission (India) for financial assistance.

- 
- [1] D. Stauffer and A. Aharony, *Introduction to Percolation Theory* (Taylor & Francis, London, 1991).
- [2] J. W. Essam, Rep. Prog. Phys. **43**, 843 (1980).
- [3] H. Kesten, *Percolation Theory for Mathematicians* (Birkhauser, Boston, 1982).
- [4] S. Galam and A. Mauger, Phys. Rev. E **53**, 2177 (1996).
- [5] J. S. Wang *et al.*, Physica A **167**, 565 (1990).
- [6] S. Kirkpatrick, Rev. Mod. Phys. **45**, 574 (1973).
- [7] J. Adler, Y. Meir, A. Aharony, A. B. Harris, and L. Klein, J. Stat. Phys. **58**, 511 (1990).
- [8] S. Feng, B. I. Halperin, and P. Sen, Phys. Rev. B **35**, 197 (1987).
- [9] E. N. Gilbert, SIAM (Soc. Ind. Appl. Math.) J. Appl. Math. **9**, 533 (1961).
- [10] S. J. Fraser and R. Kapral, J. Chem. Phys. **85**, 5682 (1986).
- [11] M. Sahimi, *Applications of Percolation Theory* (Taylor & Francis, London, 1994).
- [12] P. J. M. Bastiaansen and H. J. F. Knops, J. Phys. A **30**, 1791 (1997).
- [13] S. B. Ogale, R. Shreekala, S. I. Patil, B. Hannyoy, F. Pettit, and G. Marest (unpublished).
- [14] There is a strong belief that magnetic polarons do play a significant role in colossal magnetoresistance properties of these oxide perovskite systems [15,16]. We subscribe to this belief.
- [15] A. J. Millis, P. B. Littlewood, and B. I. Shraiman, Phys. Rev. Lett. **74**, 5144 (1995).
- [16] T. Kasuya, A. Yanase, and T. Takeda, Solid State Commun. **8**, 1551 (1970).
- [17] There exist other such equivalences for objects or obstacles with more general symmetries.
- [18] All numerical calculations have been carried out on a Silicon Graphics Workstation with a 64-bit R8000 processor and 64 Mbyte RAM.
- [19] R. E. Amritkar and Manojit Roy (unpublished).
- [20] We emphasize that our model is essentially a classical model and therefore corrections due to quantum effects are expected.
- [21] One may compare our model with continuum percolation problem [1,8]. However, it may be noted that for the physical example considered here, ours is the correct model to study it, whereas the continuum model is not physically relevant.